Construction of a *fur* null mutant and RNA-sequencing provide deeper global understanding of the *Aliivibrio salmonicida* Fur regulon

Sunniva Katharina Thode[1], Cecilie Bækkedal[1], Jenny Johansson Söderberg[1], Erik Hjerde[1], Hilde Hansen[1] and Peik Haugen[1*]

[1]Department of Chemistry and The Norwegian Structural Biology Centre, Faculty of Science and Technology, UiT − The Arctic University of Norway

*Corresponding author:

Peik Haugen[1]

Email address: peik.haugen@uit.no

Abstract

Background. The ferric uptake regulator (Fur) is a transcription factor and the main regulator of iron acquisition in prokaryotes. When bound to ferric iron, Fur recognizes its DNA binding site and generally executes its function by repressing transcription of its target genes. Due to its importance in virulence, the Fur regulon is well studied for several pathogenic model bacteria. In our previous work, we used computational predictions and microarray to gain insights into Fur-regulation in *A. salmonicida*, and have identified a number of genes and operons that appear to be under direct Fur-regulation. To provide an even more accurate and deeper global understanding of the Fur regulon we now generated an *A. salmonicida fur* knock-out strain and used RNA-sequencing to compare gene expression between the wild-type and *fur* null mutant strains.

Results. An *A. salmonicida fur* null mutant strain was constructed. Biological assays demonstrate that deletion of *fur* results in loss of fitness, with reduced growth rates and ability to withstand low-iron conditions, and oxidative stress. When comparing expression levels in the wild-type and the *fur* null mutants we retrieved 296 differentially expressed genes distributed among 18 of 21 functional classes of genes. A gene cluster encoding biosynthesis of the siderophore bisucaberin represented the highest up-regulated genes in the *fur* null mutant. Other highly up-regulated genes all encoded proteins important for iron acquisition. Potential targets for the RyhB sRNA was predicted from the list of down-regulated genes, and significant complementarities were found between RyhB and mRNAs of the *fur*, *sodB*, *cysN* and VSAL_I0422 genes. Other sRNAs with potential functions in iron homeostasis were identified.

Conclusion. The present work provides by far the most comprehensive and deepest understanding of the Fur regulon in *A. salmonicida* to date. Our data will also contribute to a better understanding of how Fur plays a key role in iron homeostasis in bacteria in general, and help to show how Fur orchestrates iron uptake when iron levels are extremely low, e.g., during the critical early phases of infections.

Keywords: *Aliivibrio salmonicida*, Fur, the ferric uptake regulator, iron homeostasis, RNA-sequencing, RyhB, gene dosage effect, small regulatory RNAs, sRNAs

Introduction

The ferric uptake regulator, Fur, represents the main regulator of iron levels in prokaryotic microorganisms (reviewed in Fillat 2014). In addition to regulating iron acquisition genes, Fur also regulate genes involved in e.g., the TCA cycle, DNA metabolism, energy metabolism, redox-stress resistance, chemotaxis, swarming, metabolic pathways, toxin production and other virulence factors, and is therefore considered as a so-called master regulator (Escolar et al. 1999; Hantke 2001; McHugh et al. 2003; Mey et al. 2005a; Pajuelo et al. 2016). Transcriptomic studies on *fur* null mutants of *Vibrio cholerae* (Mey et al. 2005a) and *Vibrio vulnificus* (Pajuelo et al. 2016) have shown that Fur represses expression of siderophore biosynthesis and transport genes, heme transport and utilization genes, ferric and ferrous iron transport genes, stress response and biofilm genes amongst others. The same studies have shown that Fur have an activating effect on genes involved in stress responses, chemotaxis, motility and toxin production. In *Escherichia coli* K-12, Fur directly regulates 131 genes including those of seven other master regulators, i.e., *flhD, flhC, felc, soxS, ryhB, rpoS* and *purR* (Keseler et al. 2013; McHugh et al. 2003), which subsequently results in regulation of 3158 genes in total (incl. direct and indirect effects) (Keseler et al. 2013). This huge number of genes translates to 70% of the total number of genes in *E. coli* K-12 (EcoCyc), and illustrates the central role of Fur in cellular processes far beyond iron homeostasis.

The 3D-structure of Fur from *Pseudomonas aeruginosa*, *E. coli*, *V. cholerae*, *Helicobacter pyroli* and *Campylobacter jejuni* is known (Butcher et al. 2012; Dian et al. 2011; Pecqueur et al. 2006; Pohl et al. 2003; Sheikh & Taylor 2009). These structures show that Fur mainly acts as a homodimer in both apo and holo forms, where at least two zinc ligands per monomer stabilize the dimer (Fillat 2014). The iron binding sites are located in a DNA binding domain of each monomer. Here, iron binding causes conformational changes that enable Fur to bind to its DNA target (known as the Fur-box) (Fillat 2014). Although several different Fur-box motifs have been proposed over the years, the current literature seems to have converged on that the Fur-box is a 19 bp palindromic sequence centered around a non-conserved nucleotide (Baichoo & Helmann 2002; Davies et al. 2011; De Lorenzo et al. 1988; Escolar et al. 1998). Once bound to its DNA target Fur mainly acts as a repressive regulator by blocking the transcription of downstream genes.

Fur activating activity was observed during early investigations of the Fur regulon and was proposed to be due to post-transcriptional regulation (Hantke 2001). The activating effect was later discovered to be due to the Fur-regulated small regulatory RNA (sRNA) named RyhB (Masse et al. 2003; Massé & Gottesman 2002; Masse et al. 2005). The apparent activating activity of Fur was found to be due to, at least in part, a secondary effects caused by *ryhB*. The RyhB sRNA is responsible for destabilizing mRNAs of its target, and repression of *ryhB* by holo-Fur was therefore interpreted as activation by Fur. RyhB typically targets iron-using or iron-binding proteins as a way of preserving the iron levels in the cell at low iron conditions (Davis et al. 2005; Masse et al. 2005; Murphy & Payne 2007). In *E. coli* RyhB directly targets 28 mRNAs (of which two encodes master regulators MarA and Fur) (EcoCyc). Other examples of RyhB targets in *E. coli* are the mRNA of *bfr, cysE, sodAB, fumA, sucBCD, icsRSUA* and *sdhABCD* (Massé & Gottesman 2002). In *V. cholerae* RyhB targets mRNAs of *sodB, sdhC, gltB1* and *fumA* and not mRNAs of iron storage genes like *bfr* and *ftn* (Davis et al. 2005).

The aim of this study was to investigate the Fur regulon in *A. salmonicida*, the causative agent of cold-water vibriosis in Atlantic salmon (*Salmo salar*), rainbow trout (*Oncorhynchus mykiss*) and Atlantic cod (*Gadus morhua*) at sea-water temperatures below 10°C (Colquhoun & Sorum 2001; Enger et al. 1991). In a previous study we identified a *Vibrionaceae*-specific Fur-box consensus as 5'- AATGANAATNATTNTCATT-3', and used computational methods to predict Fur-regulated genes and operons in four *Vibrionaceae* genomes, including *A. salmonicida* (Ahmad et al. 2009). Fur-binding motifs were associated with 60 single genes and 20 operons (89 genes). Later we used molecular dynamics (MD) simulations and binding free energy calculations to gain more insights into the interactions between *A. salmonicida* Fur (asFur) and proposed Fur-binding sites (Pedersen et al. 2010). Here, Fur-binding to promoters was dependent on the number of Fur-boxes, and the predicted "strength" (i.e., calculated similarity to Fur-box consensus) of the individual Fur-boxes. Finally, we studied Fur-regulation in *A. salmonicida* using iron-depletion experiments in combination with custom whole-genome microarray chips (Ahmad et al. 2012; Thode et al. 2015). Thirty-two genes were found to be significantly up-regulated 15 min after exposure to low-iron conditions (suggesting Fur-regulation), and interestingly, the *bibABC* genes responsible for producing the siderophore bisucaberin were identified as being most highly up-regulated (Thode et al. 2015). We have now constructed an *A. salmonicida fur* null mutant and used Illumina RNA-sequencing (RNA-seq) to compare the

transcriptomes of the wild-type strain and the *fur* null mutant. Overall, we find that the RNA-seq data overlap remarkably well with our previous findings when using microarray. However, we also show that high-throughput RNA-sequencing provide us with a much more accurate and fine-grained global understanding of the Fur regulon in *A. salmonicida*, compared to what we knew from our previous microarray work.

Material and methods

Bacterial strains, culture conditions, and sampling for RNA sequencing

A. salmonicida LFI1238 (Hjerde et al. 2008) was used as parental strain for the construction of the *A. salmonicida fur* null mutant. Parental and mutant strains were cultured in LB medium [Luria-Bertani broth Miller, Difco (later corrected to Lysogeny Broth (Bertani 2004))] containing 2.5% NaCl at 12°C and 200 rpm unless otherwise indicated. For *E. coli* strain S17-1 the growth conditions were 37°C and 200 rpm in LB medium with 1% NaCl. The suicide plasmid pDM4 was propagated in *E. coli* S17-1 cells. For selection of *E. coli* S17-1 transformants and *A. salmonicida* transconjugants, 25 µg or 2 µg of chloramphenicol/ml was added to the medium, respectively.

For RNA sequencing three biological replicates of *A. salmonicida* LFI1238 and *A.salmonicida fur* null mutant were grown in LB medium with 1% NaCl at 8°C and 200 rpm to mid log growth phase, i.e., at optical density (600 nm) of approximately 0.5. Ten mL samples were harvested, spun down and the cell pellets were then stored at -80°C for later processing.

Construction of an A. salmonicida fur *null mutant*

The *A. salmonicida fur* null mutant was constructed using the suicidal plasmid pDM4 and allelic exchange, as described by others (Milton et al. 1996). First we constructed the plasmid pDM4Δ*fur*, consisting of merged flanking regions of the *A. salmonicida fur* gene. The upstream flanking region of the *fur* gene was amplified by PCR using primers FurA forward (5'-CTACTCGAGATATTTATTTCCCTTTAATTC-3') and FurB reverse (5'-CACGTAAACTAAATATGACTTTTCCTGTATTGG-3'). For amplification of the downstream

flanking region primers FurC forward (5'-TATTTAGTTTACGTGCATAAAAAA-3') and FurD reverse (5'-CCCACTAGTATAACAAAGACTCTACTCCAG-3') were used. The resulting upstream and downstream PCR products were fused together using an overlap PCR, cut with restriction enzymes *XhoI* and *SpeI*, and ligated into the corresponding sites of pDM4. The resulting pDM4Δ*fur* construct was transformed into *E.coli* S17-1 and used as donor cells in conjugation experiments with *A. salmonicida* as described elsewhere (Bjelland et al. 2011). The allelic exchange was performed on LB agar containing 5% sucrose. The resulting *fur* null mutant was verified using PCR and DNA sequencing.

Total RNA purifications

For RNA sequencing, total RNA was purified from cell pellets using the Masterpure complete DNA & RNA purification kit (Epicentre) following the manufacturer's protocol, followed by an additional DNA removal step using the DNA-free kit (Applied Biosystems). DNase-treated total RNA was subsequently purified using the RNA cleanup RNeasy MinElute kit (Quiagen). The quality of total RNA preps was determined using a Bioanalyzer and a Prokaryote Total RNA Pico Chip (Agilent Technologies). Finally, ribosomal (r) RNA was removed from each sample (5µg total RNA) using the Ribo-Zero rRNA Removal Kit (bacteria) (Epicentre) according to the manufacturer's instructions. rRNA-depleted RNA samples were ethanol precipitated (to recover small RNAs), and analyzed on a Bioanalyzer using mRNA Pico Chips (Agilent Technologies).

RNA sequencing and data analysis

RNA-sequencing libraries were generated from purified rRNA-depleted RNA samples using the strand-specific TruSeq stranded mRNA library prep kit (Illumina), and sequenced at the Norwegian Sequencing Centre using the Illumina NextSeq 500 with mid output reagents with a read length of 75 bp and paired end reads, giving an average output of approximately 54 million reads per sample. The reads were quality checked using FastQC. Further analysis of the RNA-Seq data was performed using a Galaxy pipeline consisting of EDGE-pro v1.0.1 (Estimated Degree of Gene Expression in Prokaryotes) and DESeq. EDGE-pro was used to align the reads to

the *A. salmonicida* LFI1238 genome (Hjerde et al. 2008), and to estimate gene expression. Differences in gene expression between wild-type and *fur* null mutant were determined using DESeq. Log_2 fold changes of the genes were recalculated to × differential expression values (i.e., Δ*fur*/wt) and genes were defined as significantly differentially expressed based on a p-value ≤0.05 and differentially expression values of Δ*fur*/wt ≥2× and ≤-2×.

sRNA and mRNA target predictions

The Rockhopper software (McClure et al. 2013) was used to identify sRNA from the RNA-seq data. Input files in the analysis were fastaq files from the RNA-seq data of wild type and *fur* null mutant strains, a protein coding gene position file (.ptt), a non-coding RNA position file (.rnt), and finally genome files from *A. salmonicida* LFI1238 [NC_011312.1 (Chr I), NC_011313.1 (ChrII), NC_011311.1 (pVSAL840), NC_011314.1 (pVSAL320), NC_011315.1 (pVSAL54) and NC_011316.1 (pVSAL43)]. sRNAs identified by Rockhopper were visualized in Artemis and manually curated based on a set of criteria. To be accepted as a potential sRNA, its gene should be (i) located in an intergenic region, (ii) between 30−350 nt in length, (iii) located 30 nt or more from the nearest CDS if on the same strand, and 10 nt if on the complementary strand (based on the method of Toffano-Nioche et. al. (Toffano-Nioche et al. 2012)). RNAs fulfilling the criteria described above were further examined for presence of small open reading frames (sORF) using a method adopted from Meulen et. al. (van der Meulen et al. 2016), since there is an increasing awareness of their presence in bacterial genomes although their significance is not fully understood (Hobbs et al. 2011). Finally, EDGE-pro and DESeq was used to estimate differential gene expression levels for the sRNAs/sORFs.

TargetRNA2 and IntaRNA were used to identify potential sRNAs targets (Busch et al. 2008; Kery et al. 2014). Using sRNA sequences as queries, the programs searches for complementary regions in 5' regions of mRNAs in the *A. salmonicida* LFI1238 genome. Only targets predicted by both programs were accepted. Moreover, we also searched for mRNA targets for up-regulated sRNAs (ten sRNAs with folds Δ*fur*/wt ≥2× in the RNA-seq dataset), including RyhB, among the 34 most down-regulated genes in our RNA-seq data set. This was done to identify sRNAs with critical roles in iron homeostasis (similar to RyhB). In addition, we

predicted binding between RyhB and its known targets (*sodB, gltB, sdhC* and *fumA*) verified experimentally in *E. coli* and *V. cholerae.* Nucleotide sequences of RyhB targets from *E. coli* and *V. cholerae* were extracted from ENA. The nucleotide sequences were aligned with corresponding sequences in *A. salmonicida* and examined using Jalview.

Biological characterization of A. salmonicida fur *null mutant*

A. salmonicida LFI1238 wt and *fur* null mutant (Δ*fur*) were cultured in LB (Difco) at 8°C and 200 rpm in all experiments. Growth of cultures was monitored with optical density measured at 600nm (OD_{600nm}). To determine growth effects of *fur* null mutation, four replicates of *A. salmonicida* LF1238 wt and Δ*fur* were cultured from lag phase until stationary phase. To determine *fur* null mutation growth effects to low iron conditions, wt and Δ*fur* cultures were first grown to OD_{600nm} of 0.38 and 0.33 (mid log phase), respectively. The cultures were then split into 5 separate flasks. One culture was kept as control whereas 25−500 μM of the iron chelator 2,2'-dipyridyl was added to the remaining cultures. To determine *fur* null mutation growth effects to oxidative conditions, wt and Δ*fur* cultures were first grown OD_{600nm} of 0.4 and 0.35 (mid log phase), respectively. The cultures were then split into 5 separate flasks. One culture was kept as control whereas 50−1000 μM of hydrogen peroxide was added to the remaining cultures.

Results and discussion

Construction and basic characterization of an A. salmonicida fur *null mutant*

To better understand the Fur regulon in *A. salmonicida*, a *fur* null mutant was constructed using the genetic system described by Milton et. al. (Milton et al. 1996). Briefly, approximately 250 bp of upstream and 250 bp downstream sequences flanking the *fur* gene were merged and inserted into the pDM4 suicide vector (contains *sacBR*), then transformed into *E. coli* S17-1 cells, and finally conjugated into *A. salmonicida* LFI1238 to trigger recombination and deletion of *fur*.

Basic characterization of the *fur* null mutant was done to examine the physiological and morphological effects of the *fur* deletion. Because Fur is a global regulator, we expected the *fur*

null mutant to loose fitness due to loss of control of central cellular processes. For example, loss of Fur is expected to reduce the growth rate, and result in reduced ability to respond to external chemical stress, such as presence of H_2O_2 and iron chelators (Becerra et al. 2014; Fillat 2014; Hassett et al. 1996; Touati 2000; Yang et al. 2013). Effects on growth was monitored by comparing the growth rates of the wild-type and the *fur* null mutant in LB with 1% NaCl at 8°C and 200 rpm shaking. The OD_{600nm} of the starting cultures were set to 0.01 and then monitored until cultures reached stationary phase (typically OD_{600nm} 1.2−1.4). The lag phase for the wt and *fur* null mutant lasted approximately 10 and 35 hours, respectively, and doubling times were approximately 6 and 12 hours during mid log phase (Figure S1A and S1B). To test the ability to respond to chemical stress the *fur* null mutant and the wild-type strain were exposed to increasing concentrations of hydrogen peroxide (H_2O_2) and the iron chelator 2,2'-dipyridyl. The minimum inhibitory concentration of H_2O_2 on growth for the wild-type and *fur* null mutant were 500µM and 50µM, respectively (Figure S2A and S2B). In a similar experimental setup with 2,2'-dipyridyl the effects were less dramatic (Figure S2C and S2D). The minimum inhibitory of 2,2'-dipyridyl concentrations were similar (approx. 100µM) for both wild-type and mutant strain. However, whereas the wild-type strain grows well in the presence of 1mM 2,2'-dipyridyl, the *fur* null mutant cannot grow in the presence of 500µM.

In summary, deletion of the *fur* gene results in longer lag phase during growth, longer cell doubling time and reduced ability to respond to oxidative reagents and iron chelators. This is in agreement with results from other γ-proteobacteria model organisms (e.g., *V. vulnificus* Δ*fur* shows higher sensitivity to oxidative stress, reduced fitness and growth (Pajuelo et al. 2016) and *V. cholerae* Δ*fur* shows reduction in logarithmic growth (Mey et al. 2005a)) and support the validity of the *fur* mutant.

RNA-sequencing identifies 296 differentially expressed genes in the A. salmonicida fur *null mutant*

To provide accurate data on the Fur regulon we next compared the transcriptome of the *A. salmonicida fur* null mutant and the wild-type using an RNA sequencing approach. RNA samples (from three biological replicates) were prepared from *A. salmonicida* LFI1238 wild-type

and *fur* null mutant cells grown in LB containing 1% NaCl at 8°C to mid log phase (OD_{600nm}≈0.5). The given temperature and salt concentration were chosen because *A. salmonicida* is responsible for development of cold-water vibriosis in Atlantic salmon (i.e., at physiological salt conditions) at temperatures below 10 °C (Bergheim et al. 1990; Colquhoun & Sorum 2001). We realize that the environmental conditions the bacterium encounters inside its natural host cannot be reproduced in our experimental setup, but salt concentration and temperature are highly relevant parameters for studying factors important for development of cold-water vibriosis. RNA samples from biological replicates were subjected separately to paired-end RNA sequencing using Illumina NextSeq 500 with 75 bp read length. Sequencing generated an average output of approximately 54 million reads per sample. RNA-seq data was analyzed using a Galaxy pipeline running EDGE-pro v1.0.1 and DESeq. EDGE-pro was used to align reads to the *A. salmonicida* LFI1238 genome, and estimate gene expression. Comparison of gene expression between wild-type and *fur* null mutant were done using DESeq. Reads originating from rRNA and tRNA genes were excluded from the data analysis. Threshold values for differential expression were set to ≥2× difference (equal to Log_2=1), and with p-value≤ 0.05.

Figure 1 shows how a total of 296 differentially expressed genes are distributed among functional gene classes (functional classes based adapted from MultiFun (Serres and Riley 2000)). One hundred sixty-two and 134 genes are up-regulated and down-regulated, respectively. All functional classes, except "ribosome constituents", "nucleotide biosynthesis" and "cell division", are represented, and the two classes "cell envelope" and "transport/binding proteins" contain the highest number of genes. Considerable up-regulation of the two latter classes is expected since Fur generally regulates genes as a repressor (Fillat 2014), and loss of Fur is therefore expected to result in up-regulation (in *fur* null mutant) of genes involved in iron binding and transport over the membranes. Down-regulated genes are more evenly distributed among 18 of the 21 functional classes, including central processes such as "energy metabolism", "central metabolism", "amino acid biosynthesis" and "cell processes". Although there is no clear pattern, the combined data of up-regulated and down-regulated genes support that *as*Fur is a master regulator with functions similar to that of Fur in *E. coli* (*ec*Fur) (McHugh et al. 2003).

285 *Chromosomal distribution of differentially expressed genes*

286 Table 1 and Table 2 summarize details of genes and operons that are up- or down-regulated, and
287 Figure 2 shows the chromosomal distribution and the position of these differentially expressed
288 genes. Previous studies have shown a strong correlation between the distance of genes from *oriC*
289 (Chr I), and their general transcription level (also known as the *gene dosage effect*) (Dryselius et
290 al. 2008; Toffano-Nioche et al. 2012). That is, genes located close to *oriC* are, statistically, more
291 likely to be transcribed at higher levels than genes located further away from *oriC*, and we were
292 curious to see if *as*Fur-related genes are found clustered at specific regions of Chr I, perhaps with
293 relevance to their expression levels due to gene dosage.

294 In our experimental setup the average RPKM value for the upper half of Chr I (i.e., the region
295 closest to *ori*C) is significantly higher compared to that of the lower half (660/330 for wild-type
296 and 560/397 for *fur* null mutant). Gene dosage effects have yet to be demonstrated for Chr II
297 (Dryselius et al. 2008; Toffano-Nioche et al. 2012), which is in agreement with the RPKM values
298 in our experiment (RPKM values are similar for the upper and lower halves of the chromosome).
299 Differentially expressed genes appear to be relatively evenly distributed on the chromosome,
300 except for some clustering of genes between Chr I pos. 1.85−2.01 Mb. They represent a TonB1
301 system, heme transport and utilization, and cell envelope genes (up-regulated genes), and
302 oxidative stress response, metabolism and sRNAs (down-regulated genes). In other words, there
303 is apparently no clear pattern with respect to *as*Fur-regulated genes and their genomic position. It
304 is interesting to note, however, that the bisucaberin biosynthesis gene cluster and *ryhB* (encodes
305 the RyhB sRNA) are both located close to *oriC*. We have previously reported that the bisucaberin
306 biosynthesis system is included in the immediate response to iron limitations in *A. salmonicida*
307 (Thode et al. 2015), and its genomic location may contribute to the high level of expression and
308 fast response to iron starvation.

309

310 as*Fur regulates iron acquisition systems*

311 As expected, a high proportion of up-regulated genes (28 of 64) are directly associated with iron
312 metabolism, e.g., siderophore biosynthesis and transport, TonB systems (delivery of energy to
313 iron transport), and heme uptake and utilization. The most up-regulated (92×) gene is *bibA*,

which together with the two downstream genes *bibBC* (48× and 11× up-regulated in the *fur* null mutant, respectively) are responsible for producing the siderophore bisucaberin. Interestingly, within the large *Vibrionaceae* family *bibABC* are restricted to *A. salmonicida* and *Aliivibrio logei* (Kadi et al. 2008; Thode et al. 2015), and are in *A. salmonicida* (together with a siderophore transport system, *bitABCDE*) flanked by transposable elements (i.e., a genomic island; see (Hjerde et al. 2008)). Homology search with the BibABC amino acid sequences from *A. salmonicida*, identified that the close relative *Aliivibrio wodanis* also possess the bisucaberin biosynthesis system. The coverage and identity percentage from blastP (with *A.salmonicida* sequences used as query) were 87% identity over 100% coverage for BibA, 90% identity over 99% coverage for BibB and 89% identity over 100% coverage for BibC.

Other siderophore receptors and iron-related transport systems that are significantly up-regulated in the *fur* null mutant include the ferrichrome transport system [VSAL_II0150−0152 (6.7−12.5×)], the ferrioaxamine B receptor [VSAL_II0909 (18.8×)] and its associated ABC transporters [VSAL_II0907 (5.9×) and II0908 (18.8×)]. A siderophore ferric reductase [VSAL_II0148 (8×)] responsible for removing iron from the siderophore, the TonB1 system [VSAL_I1751−1753 (18.8−28.4×)], and finally *huvB*, *huvC* and *huvD* [VSAL_I1754−I1756 (5.8−39.7×)] responsible for heme transport, are up-regulated in the *fur* null mutant. The heme uptake and utilization gene *huvX* [VSAL_I1749 (20.2×)] and *phuW* [VSAL_I1750 (39.7×)], which encode a putative coproporphyrinogen oxidase believed to be responsible for removing iron from heme, are highly up-regulated in the *fur* null mutant. The TonB2 system [VSAL_II0110−II0116 (55.8−17.3× up-regulated)], iron(III) ABC transporters [VSAL_II0907 (5.9×) and II0908 (11.2×)] and a siderophore receptor gene *desA* [VSAL_II0909 (18.8×)] are all highly up-regulated. Interestingly, *feoABC* (VSAL_I2257−I2259) that encode the ferrous iron transport system, are apparently not strongly regulated by Fur, as only *feoC* from this system has a up-regulation ≥2× (i.e., 2.3×).

In summary, removal of the *fur* gene results in up-regulation of 28 genes directly associated with iron homeostasis (siderophore biosynthesis, transport and utilization, heme transport and utilization, ABC transporters and TonB1 and TonB2 systems) in *A. salmonicida*. *bibA* is by far the most up-regulated (92×) gene, whereas the remaining iron-relevant genes are up-regulated 55−5×.

344

345 as*Fur regulates several metal transports systems*

346 As shown in Figure 1 and Table 1, several transport systems are up-regulated in the *fur* null
347 mutant. *as*Fur may be involved in the homeostasis of other metals than iron, as multi metal
348 resistance protein genes, a multidrug efflux pump and nickel and zinc transporter genes are up-
349 regulated in the *fur* null mutant. In detail; the multi metal resistance genes *zntA* (VSAL_I2067)
350 and VSAL_II0143 are up-regulated 8.5× and 5.7×, respectively. The multidrug efflux pump
351 encoded by *vcmD* (VSAL_ I2891) is 8.5× up-regulated. A large operon (VSAL_II0118-II0125)
352 with annotated nickel and zink transporters is also up-regulated 4.1−25.7× in the *fur* null mutant.
353 Also, the outer membrane protein A gene (VSAL_I1819), a MFS transporter gene
354 (VSAL_II0149) and *potE* (VSAL_II1067) are up-regulated 5.9×, 5.6× and 5.0×, respectively.

355

356 *Down-regulated genes in asFur null mutant*

357 Fur primarily functions as a repressor. The down-regulated genes in our study (i.e., in the *fur* null
358 mutant) are expected to be positively regulated by *as*Fur in the wild-type, either via the
359 repression of *ryhB* (or other sRNAs with similar function), which typically destabilizes its mRNA
360 targets (Oglesby-Sherrouse & Murphy 2013), or by direct stimulation of expression by *as*Fur
361 itself. In this study we cannot conclusively distinguish between these two possibilities, although
362 we have predicted potential targets of RyhB and other up-regulated sRNAs (see below).

363 Table 2 shows 34 down-regulated genes in the *fur* null mutant compared to wild type.
364 Overall, the Δ*fur*/wt values for down-regulated genes are significantly lower than that of up-
365 regulated genes (the strongest down-regulation is -8.6×, when excluding *fur* that has been deleted
366 from the genome). In Table 2 we therefore present genes that are ≤ -3× down-regulated. The
367 majority of the genes are categorized as "motility/chemotaxis" or "metabolism". "Metabolism"
368 genes are involved in different pathways such as amino acid, energy, nucleotide, carbon etc.
369 Moreover, several motility and chemotaxis genes are down-regulated between -3.5× and -6.3× in
370 the *fur* null mutant. Of these, four encode flagellin subunits [*flaC-flaE* (VSAL_I2317- I2319) and
371 (*flaF* VSAL_I2517)], one encodes a sodium-type polar flagellar protein (*motX* VSAL_2771) and

two encodes methyl-accepting chemotaxis proteins (VSAL_I0799 and VSAL_I2193). Three heat shock proteins encoded by *groL1* (VSAL_I0017), *groS1* (VSAL_I0018) and *htpG* (VSAL_I0814) are also down-regulated. Heat shock proteins are involved in protein folding and unfolding, cell cycle control, transport and stress responses amongst others. Transcriptome studies of a Δ*fur* mutant in *V. vulnificus* have also shown a down-regulation of heat-shock protein genes, chemotaxis protein genes and motility-associated genes (Pajuelo et al. 2016). Two oxidative stress response protein encoding genes, *sodB* and *catA* (VSAL_I1858 and VSAL_II0215), are down-regulated in the *fur* null mutant. SodB is an iron binding protein and a RyhB target in other organisms, and CatA is a heme-binding protein.

In summary, differentially down-regulated genes in the *A. salmonicida fur* null mutant have significantly lower differential expression values (i.e., ×) than the up-regulated genes possibly due to, in part, secondary regulatory effects rather than being directly regulated by Fur. The majority of down-regulated genes have functions in chemotaxis, motility, heat shock and oxidative stress response.

Identification of sRNAs with roles in iron homeostasis

ncRNAs represent an important part of regulons in bacteria, often controlling critical and early steps in regulatory pathways (Gottesman 2005). We therefore set out to explore the presence and function of sRNAs in our RNA-seq dataset. Table 1 already showed us that *ryhB* is up-regulated 43× in the *fur* null mutant, which strongly supports that RyhB in *A. salmonicida* has a similar role in iron homeostasis as what was established for its homologs in e.g., *E. coli* (Masse et al. 2005) and *V. cholerae* (Davis et al. 2005). Here, RyhB is produced under low-iron conditions and stops production of iron-using/storing proteins, and therefore contributes to a lowered demand for iron.

To search for other sRNAs with potential roles in iron homeostasis we re-analyzed the RNA-seq dataset. The rational was that any Fur-regulated sRNA gene are likely candidates to have roles in iron metabolism by targeting specific mRNAs for degradation. One sRNA gene (VSAL_II2005s) that fulfilled this criterion was identified among 252 sRNA genes that we predicted in a previous work (Ahmad et al. 2012). VSAL_II2005s was up-regulated 4×. Furthermore, we analyzed the RNA-seq data using Rockhopper. Rockhopper predicts ncRNAs from RNA-seq data. The sRNA predicted by Rockhopper were manually curated using the

Artemis software. Briefly, to be accepted as a true sRNA, its gene had to be (i) located in an intergenic region, (ii) between 30−350 nt in length, (iii) located 30 nt or more from the nearest CDS if on the same strand, and 10 nt if on the complementary strand.

Ninety-three potential sRNA were predicted using Rockhopper, including predictions of sRNAs in pseudogene regions. Seventeen were kept after manual curation, eight of which overlapped or were complementary to previously predicted sRNAs in *A. salmonicida* (Ahmad et al. 2012). These eight sRNAs were VSAL_I4057s, VSAL_I4069s and VSAL_I4164s (overlapping), and VSAL_I4107s, VSAL_I4164s, VSAL_I4189s, VSAL_II2008s and VSAL_II2050s (complementary). Of the remaining nine new sRNAs identified by Rockhopper and manual curation, six are located on Chr I and three on Chr II (see Table 3). New sRNAs 4 and 7 both contain sORFs, which potentially encode small proteins (see Material and methods) (Hobbs et al. 2011). The nine new sRNA were added to the *A. salmonicida* genome annotation using Artemis, and the RNA-seq data was re-analyzed for differentially expressed genes using EDGE-pro and DESeq. Two of the new sRNAs, i.e., number 1 and 9, were up-regulated 2.2× and 2.5× in the *fur* null mutant, respectively. Homology searches did not give significant hits.

In summary, RyhB and a previously predicted sRNA (VSAL_II2005s) were up-regulated in the *A. salmonicida fur* null mutant. Nine new sRNAs were predicted using Rockhopper and manual curation, of which two were differentially expressed (i.e., number 1 and 9 in Table 3).

sRNA target predictions

Next, we used the TargetRNA2 and IntaRNA softwares to test if the up-regulated sRNAs identified above can explain some of the down-regulated protein-coding genes. The up-regulated sRNAs *ryhB*, VSAL_II2005s and new sRNAs 1 and 9 (Table 3) were tested for target binding towards the 34 down-regulated genes presented in Table 2. *ryhB* is up-regulated 43.7×, and typically targets mRNA for iron using and iron storage proteins (Davis et al. 2005; Masse et al. 2005; Mey et al. 2005b; Murphy & Payne 2007; Oglesby-Sherrouse & Murphy 2013). We expected to find same/ similar targets in our datasets. RyhB target predictions suggests that seven of the mRNAs listed in Table 2 have significant complementarity to RyhB. Two of the corresponding genes, i.e., *sodB* and *fur*, represent known targets from other organisms (Davis et al. 2005; Masse et al. 2005; Mey et al. 2005b). The other identified targets are *cysN*

(VSAL_I0421), VSAL_I0422, *tcyP* (VSAL_I1813), VSAL_II1026 and VSAL_I0424. Furthermore, we tested other known targets for complementarity to RyhB. Matches were found to *gltB* and *sdhC*, which were down-regulated 2.1× and 1.3×, respectively. We therefore consider *gltB* as a potential RyhB target in *A. salmonicida*, while *sdhC* is probably not due to the weak regulation. In *E. coli* K-12, GltB is an iron-sulfur binding protein. Thus, down-regulation of *gltB* is an iron sparing strategy.

Our target predictions for VSAL_II2005s (which was 4× up-regulated) suggest significant complementarity to *tcyP* (VSAL_I1813). Interestingly, *tcyP* was also identified as a RyhB target, which may explain why *tcyP* has a relative strong down-regulation of -8.6× (when compared to the other down-regulated genes) in the *fur* null mutant. No potential targets were identified for the new sRNAs 1 and 9.

In summary, *as*RyhB appears to have similar regulatory functions as its known homologs from other model organisms, and may account for the down-regulation of seven of the 34 genes in Table 2. We also identified *tcyP* as a potential target for both RyhB and VSAL_II2005s. No complementatrity was found between the new sRNAs 1 and 9 and mRNAs corresponding to the down-regulated genes listed in Table 2.

Concluding remarks

We have studied the Fur regulon of *A. salmonicida* using gene knock out technology and compared the transcriptome of the *fur* null mutant with its isogeneic wild type using RNA sequencing. Our results show that *as*Fur acts as a master regulator in *A. salmonicida* affecting ~7% of the CDSs, when threshold values were set to 2× differential expression and with p-values ≤ 0.05. We also demonstrate that *as*Fur acts mainly as a repressor. This conclusion is based on that Δ*fur*/wt differential expression values of up-regulated genes in the *fur* null mutant are significantly higher than that of down-regulated genes. Furthermore, we demonstrated a strong *gene dosage effect* for Chr I. This result adds to the growing list of *Vibrionaceae* bacteria where the transcription level is, statistically, highest in the chromosomal regions surrounding the *oriC*, and weaker for genes located further away from *Ori*C. Finally, we identify sRNAs with potential roles in iron homeostasis. The role for RyhB is well established, and in addition we identify VSAL_II2005s, which was 4× up-regulated in a fur null mutant, as another sRNA that contains significant complementarity to *tcyP* (VSAL_I1813).

Our current data is in good overall agreement with our previous work (Ahmad et al. 2012; Ahmad et al. 2009; Pedersen et al. 2010; Thode et al. 2015). As expected, we found a large overlap in data between experiments where *A. salmonicida* was subjected to low-iron conditions and global changes in gene expression was monitored using microarray (Thode et al. 2015), and this work where the global gene expression data (using RNA-seq) of a *fur* null mutant and wild type strain were compared. Of the 32 genes identified by microarray, 4 are not ≥2x up-regulated in the *fur* null mutant (i.e., *feoA, feoB,* VSAL_II0717 and VSAL_I2980), while the remaining 28 are ≥2× up-regulated. With the latest data we conclude that we today have a more accurate and fine-grained global understanding of how *A. salmonicida* regulates gene expression under low-iron conditions, which is a highly relevant setting that the bacterium is expected to confront during initial phases of infection of Atlantic salmon. In the future, we will shift our focus from basic knowledge of bacterial iron metabolism towards how this can be applied to the benefit of society. Possible directions could be using microbial iron metabolism systems as targets for new antimicrobial drugs and/or production of iron scavenging molecules that could be useful in medicine and agriculture (Saha et al. 2013, Gorska et al. 2014).

Availability of supporting data

RNA sequencing data are available in the European Nucleotide Archive (ENA) under accession number PRJEB17700.

Additional files

Figure S1. Linear and logarithmic growth curves of *A. salmonicida* LFI1238 wt and *fur* null mutant.

Figure S2. Chemical titration test of *A. salmonicida* LFI1238 wt and *fur* null mutant.

Abbreviations

ABC transporter: ATP-binding cassette; Fur: Ferric Uptake Regulator; *ec*Fur: *Escherichia coli* Fur; *as*Fur: *Aliivibrio salmonicida* Fur; sRNA: small regulatory RNA; ORF: Open reading frame; mRNA: messenger RNA; TCA: tricarboxylic acid; DNA: Deoxyribonucleic acid; RNA: Ribonucleic acid; bp: base pair; nt: nucleotide; LB: Luria Bertani broth/ Lysogen Broth; tRNA: transfer RNA; rRNA: ribosomal RNA; Chr: Chromosome; MFS transporter: major facilitator superfamily transporter; h: hours; PCR: Polymerase Chain Reaction; OD: optical density; wt: wild type; RPKM: reads per kilo base per million reads; RNA-seq: RNA sequencing; rpm: rounds per minute; *AS*: *Aliivibrio salmonicida*; sORF: small open reading frame; ncRNA: non coding RNA; Δ*fur*: *fur* null mutant.

Acknowledgments

The sequencing service was provided by the Norwegian Sequencing Centre (www.sequencing.uio.no), a national technology platform hosted by the University of Oslo and supported by the "Functional Genomics" and "Infrastructure" programs of the Research Council of Norway and the Southeastern Regional Health Authorities.

Competing interests

The authors declare that they have no competing interests.

Ethics statement

The research presented in this paper do not involve human subjects, and we see no ethical issues.

Authors` contributions

PH, HH and SKT conceived the study and designed experiments. HH supervised and participated in the construction of the *fur* null mutant, and PH supervised the studies and helped draft the manuscript. SKT performed the construction of the *fur* null mutant, biological characterizations,

cultured samples for RNA sequencing, total RNA purifications, post analysis of the RNA-seq data and drafted the manuscript. CB performed the RNA-seq data analysis, expression analysis, sRNA and mRNA target predictions and drafted the manuscript. EH supervised the data analysis, provided and helped adjust scripts, and deposited the data to ENA. JS performed quality testing and rRNA depletion of the RNA. All authors read and approved the final manuscript.

References

EcoCyc. *Available at http://ecocyc.org/* (accessed 09.22.16 2016).

Ahmad R, Hansen GÅ, Hansen H, Hjerde E, Pedersen HL, Paulsen SM, Nyrud MLJ, Strauss A, Willassen NP, and Haugen P. 2012. Prediction, Microarray and Northern Blot Analyses Identify New Intergenic Small RNAs in *Aliivibrio salmonicida*. *J Mol Microb Biotech* 22:352-360.

Ahmad R, Hjerde E, Hansen G, Haugen P, and Willassen N. 2009. Prediction and experimental testing of ferric uptake regulator regulons in vibrios. *J Mol Microbiol Biotechnol* 16:159 - 168.

Baichoo N, and Helmann J. 2002. Recognition of DNA by Fur: a reinterpretation of the Fur box consensus sequence. *J Bacteriol* 184:5826 - 5832.

Becerra G, Merchán F, Blasco R, and Igeño MI. 2014. Characterization of a ferric uptake regulator (Fur)-mutant of the cyanotrophic bacterium *Pseudomonas pseudoalcaligenes* CECT5344. *J Biotechnol* 190:2-10.

Bergheim A, Kroglund F, Vatne D, and Rosseland B. 1990. Blood plasma parameters in farmed Atlantic salmon (*Salmo salar* L.) transferred to sea cages at age eight to ten months. *Aquaculture* 84:159 - 165.

Bertani G. 2004. Lysogeny at Mid-Twentieth Century: P1, P2, and Other Experimental Systems. *J Bacteriol* 186:595-600.

Busch A, Richter AS, and Backofen R. 2008. IntaRNA: efficient prediction of bacterial sRNA targets incorporating target site accessibility and seed regions. *Bioinformatics* 24:2849-2856.

Butcher J, Sarvan S, Brunzelle JS, Couture JF, and Stintzi A. 2012. Structure and regulon of *Campylobacter jejuni* ferric uptake regulator Fur define apo-Fur regulation. *Proc Natl Acad Sci U S A* 109:10047-10052.

Colquhoun D, and Sorum H. 2001. Temperature dependent siderophore production in *Vibrio salmonicida*. *Microb Pathog* 31:213 - 219.

Davies B, Bogard R, and Mekalanos J. 2011. Mapping the regulon of *Vibrio cholerae* ferric uptake regulator expands its known network of gene regulation. *Proc Natl Acad Sci U S A* 108:12467 - 12472.

Davis B, Quinones M, Pratt J, Ding Y, and Waldor M. 2005. Characterization of the small untranslated RNA RyhB and its regulon in *Vibrio cholerae*. *J Bacteriol* 187:4005 - 4014.

De Lorenzo V, Giovannini F, Herrero M, and Neilands J. 1988. Metal ion regulation of gene expression: Fur repressor-operator interaction at the promoter region of the aerobactin system of pCoIV-K30. *J Mol Biol* 203:875 - 884.

Dian C, Vitale S, Leonard GA, Bahlawane C, Fauquant C, Leduc D, Muller C, de Reuse H, Michaud-Soret I, and Terradot L. 2011. The structure of the *Helicobacter pylori* ferric uptake regulator Fur reveals three functional metal binding sites. *Mol Microbiol* 79:1260-1275.

557 Dryselius R, Izutsu K, Honda T, and Iida T. 2008. Differential replication dynamics for large and small
558 Vibrio chromosomes affect gene dosage, expression and location. *BMC Genomics* 9:1-16.
559 Enger O, Husevag B, and Goksoyr J. 1991. Seasonal variations in precense of *Vibrio salmonicida* and total
560 bacterial counts in Norwegian fish-farm water. *Can J Microbiol* 37:618 - 623.
561 Escolar L, Perez-Martin J, and de Lorenzo V. 1998. Binding of the fur (ferric uptake regulator) repressor of
562 *Escherichia coli* to arrays of the GATAAT sequence. *J Mol Biol* 283:537-547.
563 Escolar L, Perez-Martin J, and de Lorenzo V. 1999. Opening the Iron Box: Transcriptional
564 Metalloregulation by the Fur Protein. *J Bacteriol* 181:6223-6229.
565 Fillat MF. 2014. The FUR (ferric uptake regulator) superfamily: Diversity and versatility of key
566 transcriptional regulators. *Arch Biochem Biophys* 546:41-52.
567 Gorska A, Sloderbach A, and Marszall MP. 2014. Siderophore-drug complexes: potential medicinal
568 applications of the 'Trojan horse' strategy. *Trends Pharmacol Sci* 35:442-449.
569 10.1016/j.tips.2014.06.007
570 Gottesman S. 2005. Micros for microbes: non-coding regulatory RNAs in bacteria. *Trends Genet* 21:399-
571 404.
572 Hantke K. 2001. Iron and metal regulation in bacteria. *Curr Opin Microbiol* 4:172 - 177.
573 Hassett DJ, Sokol PA, Howell ML, Ma JF, Schweizer HT, Ochsner U, and Vasil ML. 1996. Ferric uptake
574 regulator (Fur) mutants of *Pseudomonas aeruginosa* demonstrate defective siderophore-
575 mediated iron uptake, altered aerobic growth, and decreased superoxide dismutase and catalase
576 activities. *J Bacteriol* 178:3996-4003.
577 Hjerde E, Lorentzen M, Holden M, Seeger K, Paulsen S, and Bason N. 2008. The genome sequence of the
578 fish pathogen *Aliivibrio salmonicida* strain LFI1238 shows extensive evidence of gene decay. *BMC*
579 *Genomics* 9:616.
580 Hobbs EC, Fontaine F, Yin X, and Storz G. 2011. An expanding universe of small proteins. *Curr Opin*
581 *Microbiol* 14:167-173.
582 Kadi N, Song L, and Challis G. 2008. Bisucaberin biosynthesis: an adenylating domain of the BibC multi-
583 enzyme catalyzes cyclodimerization of N-hydroxy-N-succinylcadaverine. *Chem Commun (Camb)*
584 41:5119 - 5121.
585 Kery MB, Feldman M, Livny J, and Tjaden B. 2014. TargetRNA2: identifying targets of small regulatory
586 RNAs in bacteria. *Nucleic Acids Res* 42:W124-W129.
587 Keseler IM, Mackie A, Peralta-Gil M, Santos-Zavaleta A, Gama-Castro S, Bonavides-Martínez C, Fulcher C,
588 Huerta AM, Kothari A, Krummenacker M, Latendresse M, Muñiz-Rascado L, Ong Q, Paley S,
589 Schröder I, Shearer AG, Subhraveti P, Travers M, Weerasinghe D, Weiss V, Collado-Vides J,
590 Gunsalus RP, Paulsen I, and Karp PD. 2013. EcoCyc: fusing model organism databases with
591 systems biology. *Nucleic Acids Res* 41:D605-D612.
592 Masse E, Escorcia FE, and Gottesman S. 2003. Coupled degradation of a small regulatory RNA and its
593 mRNA targets in *Escherichia coli*. *Genes Dev* 17:2374-2383.
594 Massé E, and Gottesman S. 2002. A small RNA regulates the expression of genes involved in iron
595 metabolism in *Escherichia coli*. *P Nat Acad Sci* 99:4620-4625.
596 Masse E, Vanderpool C, and Gottesman S. 2005. Effect of RyhB small RNA on global iron use in
597 *Escherichia coli*. *J Bacteriol* 187:6962 - 6971.
598 McClure R, Balasubramanian D, Sun Y, Bobrovskyy M, Sumby P, Genco CA, Vanderpool CK, and Tjaden B.
599 2013. Computational analysis of bacterial RNA-Seq data. *Nucleic Acids Res* 41:e140.
600 McHugh J, Rodriguez-Quinones F, Abdul-Tehrani H, Svistunenko D, Poole R, and Cooper C. 2003. Global
601 iron-dependent gene regulation in *Escherichia coli*. *J Biological Chem* 278:29478 - 29486.
602 Mey A, Wyckoff E, Kanukurthy V, Fisher C, and Payne S. 2005a. Iron and Fur regulation in *Vibrio cholerae*
603 and the role of Fur in virulence. *Infect Immun* 73:8167 - 8178.

Mey AR, Craig SA, and Payne SM. 2005b. Characterization of *Vibrio cholerae* RyhB: the RyhB Regulon and Role of ryhB in Biofilm Formation. *Infect Immun* 73:5706-5719.
Milton DL, O'Toole R, Horstedt P, and Wolf-Watz H. 1996. Flagellin A is essential for the virulence of *Vibrio anguillarum*. *J Bacteriol* 178.
Murphy ER, and Payne SM. 2007. RyhB, an Iron-Responsive Small RNA Molecule, Regulates *Shigella dysenteriae* Virulence. *Infect Immun* 75:3470-3477.
Oglesby-Sherrouse AG, and Murphy ER. 2013. Iron-Responsive Bacterial Small RNAs: Variations on a Theme. *Metallomics* 5:276-286.
Pajuelo D, Hernandez-Cabanyero C, Sanjuan E, Lee CT, Silva-Hernandez FX, Hor LI, MacKenzie S, and Amaro C. 2016. Iron and Fur in the life cycle of the zoonotic pathogen *Vibrio vulnificus*. *Environ Microbiol*.
Pecqueur L, D'Autreaux B, Dupuy J, Nicolet Y, Jacquamet L, Brutscher B, Michaud-Soret I, and Bersch B. 2006. Structural changes of *Escherichia coli* ferric uptake regulator during metal-dependent dimerization and activation explored by NMR and X-ray crystallography. *J Biol Chem* 281:21286-21295.
Pedersen HL, Ahmad R, Riise EK, Leiros HK, Hauglid S, Espelid S, Brandsdal BO, Leiros I, Willassen NP, and Haugen P. 2010. Experimental and computational characterization of the ferric uptake regulator from *Aliivibrio salmonicida* (*Vibrio salmonicida*). *J Microbiol* 48:174-183.
Pohl E, Haller JC, Mijovilovich A, Meyer-Klaucke W, Garman E, and Vasil ML. 2003. Architecture of a protein central to iron homeostasis: crystal structure and spectroscopic analysis of the ferric uptake regulator. *Mol Microbiol* 47:903-915.
Saha R, Saha N, Donofrio RS, and Bestervelt LL. 2013. Microbial siderophores: a mini review. *J Basic Microbiol* 53:303-317.
Serres MH, Riley M. 2000. MultiFun, a multifunctional classification scheme for *Escherichia coli* K-12 gene products. *Microb Comp Genomics*. 5:205-222.
Sheikh M, and Taylor G. 2009. Crystal structure of the *Vibrio cholerae* ferric uptake regulator (Fur) reveals insights into metal co-ordination. *Mol Microbiol* 72:1208 - 1220.
Thode SK, Kahlke T, Robertsen EM, Hansen H, and Haugen P. 2015. The immediate global responses of *Aliivibrio salmonicida* to iron limitations. *BMC Microbiol* 15:1-9.
Toffano-Nioche C, Nguyen AN, Kuchly C, Ott A, Gautheret D, Bouloc P, and Jacq A. 2012. Transcriptomic profiling of the oyster pathogen *Vibrio splendidus* opens a window on the evolutionary dynamics of the small RNA repertoire in the Vibrio genus. *RNA* 18:2201-2219.
Touati D. 2000. Iron and oxidative stress in bacteria. *Arch of Biochem Biophys* 373:1 - 6.
van der Meulen SB, de Jong A, and Kok J. 2016. Transcriptome landscape of *Lactococcus lactis* reveals many novel RNAs including a small regulatory RNA involved in carbon uptake and metabolism. *RNA Biol* 13:353-366.
Yang X-W, He Y, Xu J, Xiao X, and Wang F-P. 2013. The Regulatory Role of Ferric Uptake Regulator (Fur) during Anaerobic Respiration of *Shewanella piezotolerans* WP3. *PLoS ONE* 8:e75588.

Tables

Table 1: Up-regulated (≥4×) genes in *A. salmonicida fur* null mutant compared to wild type.

VSAL_nr	*gene*	Annotation	*Δfur*/ wt	Fur-box**
Siderophore biosynthesis and transport				
VSAL_I0134 *	*bibA*	Bisucaberin siderophore biosynteshis protein A	92.6	x
VSAL_I0135	*bibB*	Bisucaberin siderophore biosynteshis protein B	48.2	x
VSAL_I0136	*bibC*	Bisucaberin siderophore biosynteshis protein C	11.1	x
VSAL_I0137	*bitA*	TonB-dependent iron-siderophore receptor precursor	9.3	x
VSAL_II0148		2Fe-2S binding protein, siderophore ferric reductase	8.0	x
VSAL_II0150	*fhuC*	ferrichrome transport ATP-binding protein FhuC	7.0	x
VSAL_II0151	*fhuD*	ferrichrome-binding periplasmic protein	12.5	x
VSAL_II0152	*fhuB*	ferrichrome transport protein FhuB	6.7	x
VSAL_II0907		iron(III) ABC transporter, periplasmic iron-compound-binding (pseudo)	5.9	x
VSAL_II0908	*hatC*	iron(III) ABC transporter, ATP-binding protein	11.2	x
VSAL_II0909	*desA*	ferrioxamine B receptor	18.8	x
TonB systems				
VSAL_I1751	*tonB1*	TonB protein (pseudogene)	18.8	x
VSAL_I1752	*exbB1*	TonB system transport protein ExbB1	25.2	x
VSAL_I1753	*exbD1*	TonB system transport protein ExbD1	28.4	x
VSAL_II0110		TonB dependent receptor	55.8	x
VSAL_II0111		putative exported protein	35.3	x
VSAL_II0112	*tolR2*	biopolymer transport protein TolR	25.7	x
VSAL_II0113	*exbB2*	TonB system transport protein ExbB2	17.3	x
VSAL_II0114	*exbD2*	TonB system transport protein ExbD2	27.6	x
VSAL_II0115	*tonB2*	TonB protein	30.1	x
VSAL_II0116		putative exported protein	23.4	x
Heme uptake and utilization				
VSAL_I1734		heme receptor (pseudogene)	6.6	x
VSAL_I1749	*huvX*	heme uptake and utilization protein HuvX	20.2	x
VSAL_I1750	*phuW*	putative coproporphyrinogen oxidase PhuW	39.7	x
VSAL_I1754	*huvB*	heme transporter protein HuvB, periplasmic binding protein	39.7	x
VSAL_I1755	*huvC*	heme transporter protein HuvC, transmembrane permease component	13.5	x
VSAL_I1756	*huvD*	heme transporter protein HuvD, ATP-binding component	5.8	x
small RNA				
VSAL_I3102s	*ryhB*	small RNA RyhB	43.7	x
VSAL_II2005s		VSAsRNA006	4.0	
Other transport				

VSAL_I1819		outer membrane protein A	5.9	
VSAL_I2067	*zntA*	lead, cadmium, zinc and mercury-transporting ATPase	8.5	
VSAL_I2891	*vcmD*	multidrug efflux pump	8.5	x
VSAL_II0118		membrane protein	16.9	
VSAL_II0119		putative exported protein	25.7	
VSAL_II0120		nickel transporter	16.7	
VSAL_II0121		putative exported protein	16.7	
VSAL_II0122		putative membrane protein	8.7	
VSAL_II0123		zinc ABC transporter periplasmic substrate binding protein	7.4	
VSAL_II0124		zinc ABC transporter ATP binding protein	6.3	
VSAL_II0125		zinc ABC transporter permease	4.1	
VSAL_II0149		MFS transporter	5.6	
VSAL_II1043		cation efflux pump, cobalt-zinc-cadmium resistance protein	5.7	
VSAL_II1067	*potE*	putrescine-ornithine antiporter	5.0	
Metabolism				
VSAL_I1785		thiol oxioreductase	5.7	
VSAL_I1786		peptidase, putative iron-regulated	8.2	x
VSAL_I2892		methyltransferase	12.4	x
VSAL_II0932	*bcsA*	cellulose synthase catalytic subunit	6.1	
VSAL_II1066	*speF*	ornithine decarboxylase, inducible	7.4	
Cell envelope				
VSAL_I1328		putative membrane associated peptidase	4.4	
VSAL_I1783		putative lipoprotein	4.4	
VSAL_I1784		putative lipoprotein	5.0	
VSAL_I1820		putative lipoprotein	4.0	
VSAL_I1864		putative membrane protein	20.1	x
VSAL_II0074		membrane protein	67.3	x
VSAL_II0868		putative lipoprotein	8.0	x
VSAL_II0931		membrane protein (fragment)	4.8	
VSAL_II0933		putative exported protein	6.2	
VSAL_II0937		membrane protein	4.0	
Unknown function				
VSAL_I0881		putative exported protein	15.7	x
VSAL_I0882		putative exported protein	14.1	x
VSAL_I0883		putative exported protein	14.4	x
VSAL_I0884		putative exported protein	5.0	x
VSAL_II0469		hypothetical protein	4.5	
VSAL_II0934		hypothetical protein	4.0	

* p-value not analyzed

** fur-box predictions from Ahmad et.al. (Ahmad et al. 2009)

649 **Table 2:** Down-regulated (≤ -3×) genes in *A. salmonicida fur* null mutant compared to wild type.

VSAL_nr	*gene*	annotation	*Δfur/* wt	sRNA target
Motility/ chemotaxis				
VSAL_I0799		methyl-accepting chemotaxis protein	-3.5	
VSAL_I2193*		methyl-accepting chemotaxis protein	-3.6	
VSAL_I2317	*flaE*	flaggelin subunit E	-5.1	
VSAL_I2318	*flaD*	flaggelin subunit D	-4.3	
VSAL_I2319	*flaC*	flaggelin subunit C	-6.2	
VSAL_I2517	*flaF*	flaggelin subunit F	-3.9	
VSAL_I2771	*motX*	sodium-type polar flagellar protein MotX	-5.0	
Oxidative stress response				
VSAL_I1858	*sodB*	superoxide dismutase [Fe]	-3.1	RyhB
VSAL_II0215	*catA*	catalase	-3.4	
Metabolism				
VSAL_I0122	*prlC*	oligopeptidase A	-3.2	
VSAL_I0421	*cysN*	sulfate adenylyltransferase subunit 1	-3.4	RyhB
VSAL_I0422		ion transporter superfamily protein	-3.8	RyhB
VSAL_I0423	*cysC*	adenylylsulfate kinase	-4.0	
VSAL_I1133	*hisG*	ATP phosphoribosyltransferase	-3.4	
VSAL_I1769	*nrdA*	ribonucleoside-diphosphate reductase 1 alpha chain	-3.8	
VSAL_I1857	*queD*	queuosine biosynthesis protein	-4.0	
VSAL_II0666	*idnK*	thermosensitive gluconokinase	-4.4	
VSAL_II0846		putative acetyltransferase	-3.4	
VSAL_II1026		putative tryptophanyl-tRNA synthetase	-6.4	RyhB
small RNA				
VSAL_I4000s		VSsRNA001	-4.1	
VSAL_I4069s		VSsRNA070	-3.4	
VSAL_I4100s		VSsRNA 101	-4.1	
VSAL_I4139s		VSsRNA140	-3.9	
Chaperones/ heat shock proteins				
VSAL_I0017	*groL1*	60 kda chaperonin 1	-3.2	
VSAL_I0018	*groS1*	10 kDa chaperonin 1	-3.9	
VSAL_I0814	*htpG*	chaperone protein HtpG (heat shock protein HtpG)	-3.2	
Cell envelope/ transport				
VSAL_I1813	*tcyP*	L-cystine transporter	-8.6	RyhB, VSAL_II2005s
VSAL_II0853		MFS transporter	-4.0	
VSAL_II0854		secretion protein, HlyD family	-3.9	
VSAL_II1062		membrane protein	-3.3	
Unknown function				

VSAL_I0424		hypothetical protein	-3.2	RyhB
VSAL_I2064		conserved hypothetical protein	-4.0	
VSAL_II0168		putative exported protein	-7.9	
Mutated gene/ control gene				
VSAL_I0833	*fur*	ferric uptake regulator protein	-128.7	RyhB

*fur-box predicted in Ahmad et. al. (Ahmad et al. 2009)

650

651

652 **Table 3:** sRNAs identified by Rockhopper.

New sRNA	Start bp	Stop bp	Length	Flanking upstream	Flanking downstream	Strand	Possible sORF	*Δfur*/wt RNA seq	p-value RNA seq
1	51134	51393	259	VSAL_I0047	VSAL_I0048	+	no	2.22	0
2	776673	776837	164	VSAL_I0690	VSAL_I0691	+	no	-1.27	0.41
3	2343220	2343291	71	VSAL_I2181	VSAL_I2182	+	no	1.21	0.15
4	2405357	2405638	281	VSAL_I2233	VSAL_I2234	+	yes	1.06	0.66
5	2812966	2813103	137	VSAL_I3191r	VSAL_I2601	+	no	-1.52	0.18
6	3259173	3259344	171	VSAL_I3008	VSAL_I3009	-	no	-1.05	0.69
7	692443	692539	96	VSAL_II0641	VSAL_II0642	+	yes	1.97	0.01
8	814013	814056	43	VSAL_II2035s	VSAL_II0738	-	no	-1.05	0.85
9	1141984	1142209	225	VSAL_II1046	VSAL_II1047	+	no	2.53	0.00

653

654

655

656

657

658

659

660

661

662

Figure legends

Figure 1. Functional distribution of genes that are ≥2× differentially expressed between *A. salmonicida* wild type and the *fur* null mutant strain. The number in parenthesis represent the percentage of the total number of genes within the genome in each functional class.

Figure 2. Schematic circular diagrams of the *A. salmonicida* chromosomes I and II (ChrI and ChrII). Circles indicate from outside to inside differentially expressed genes ≥4× (indicated with light blue filled circles) and ≤ -3× (indicated with orange filled circles), the scale in base-pairs, CDSs on leading strand (green), CDSs on lagging strand (blue), non-coding RNA genes [sRNAs (red), tRNAs and rRNAs (grey)], differential expression in *fur* null mutant compared to wild-type strain (up-regulation is shown in green bars, down-regulation in red bars), amount of RNA-seq reads mapped to the chromosome in *fur* null mutant (blue bars) and wild-type (red bars) strain. Figure is not to scale.

Figure S1. Linear (A) and logarithmic (B) growth curves of *A. salmonicida* LFI1238 wt and *fur* null mutant grown in LB containing 1% NaCl, at 8°C with 200 rpm agitation. Four biological replicates were used. Grey area indicate the measured span and dotted line indicate the average curve.

Figure S2. Chemical titration test of *A. salmonicida* LFI1238 wt and *fur* null mutant. Growth conditions were LB containing 1% NaCl, at 8°C with 200 rpm agitation. The cultures were grown to mid-log phase, split to smaller cultures and added increasing amounts of H_2O_2 and 2,2'-dipyridyl. A) *AS* wt grown with increasing concentrations of H_2O_2. B) *AS* Δ*fur* grown with increasing concentrations of H_2O_2. C) *AS* wt grown with increasing concentrations of 2,2'-dipyridyl. D) *AS* Δ*fur* grown with increasing concentrations of 2,2'-dipyridyl.

Figure 1

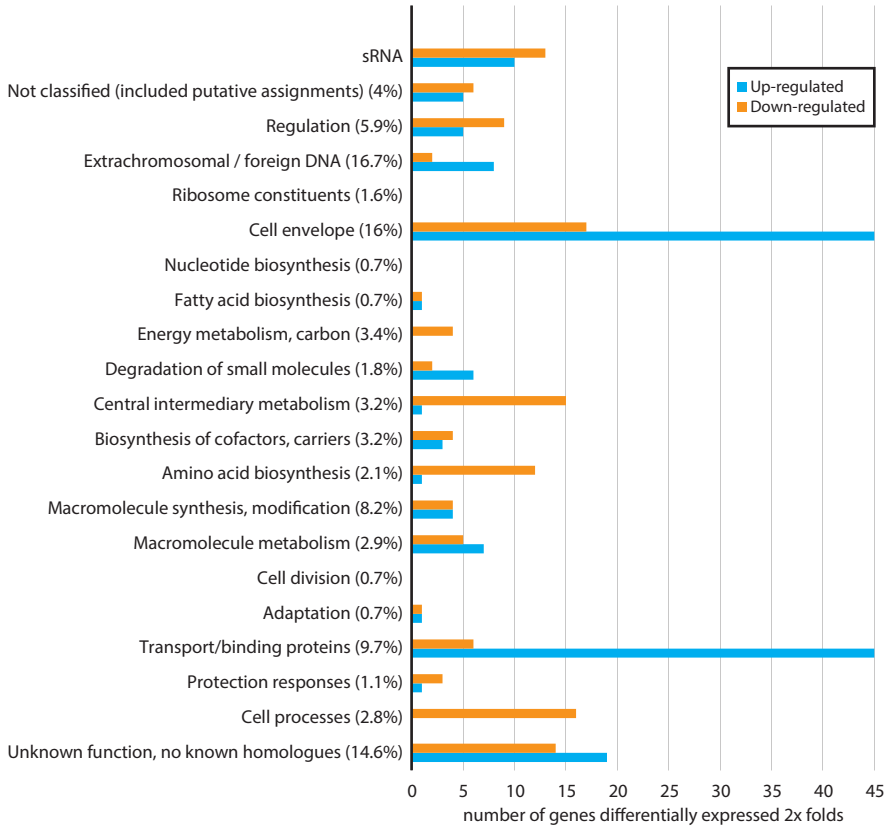
sRNA
Not classified (included putative assignments) (4%)
Regulation (5.9%)
Extrachromosomal / foreign DNA (16.7%)
Ribosome constituents (1.6%)
Cell envelope (16%)
Nucleotide biosynthesis (0.7%)
Fatty acid biosynthesis (0.7%)
Energy metabolism, carbon (3.4%)
Degradation of small molecules (1.8%)
Central intermediary metabolism (3.2%)
Biosynthesis of cofactors, carriers (3.2%)
Amino acid biosynthesis (2.1%)
Macromolecule synthesis, modification (8.2%)
Macromolecule metabolism (2.9%)
Cell division (0.7%)
Adaptation (0.7%)
Transport/binding proteins (9.7%)
Protection responses (1.1%)
Cell processes (2.8%)
Unknown function, no known homologues (14.6%)
Up-regulated
Down-regulated
0 5 10 15 20 25 30 35 40 45
number of genes differentially expressed 2x folds

Figure 2

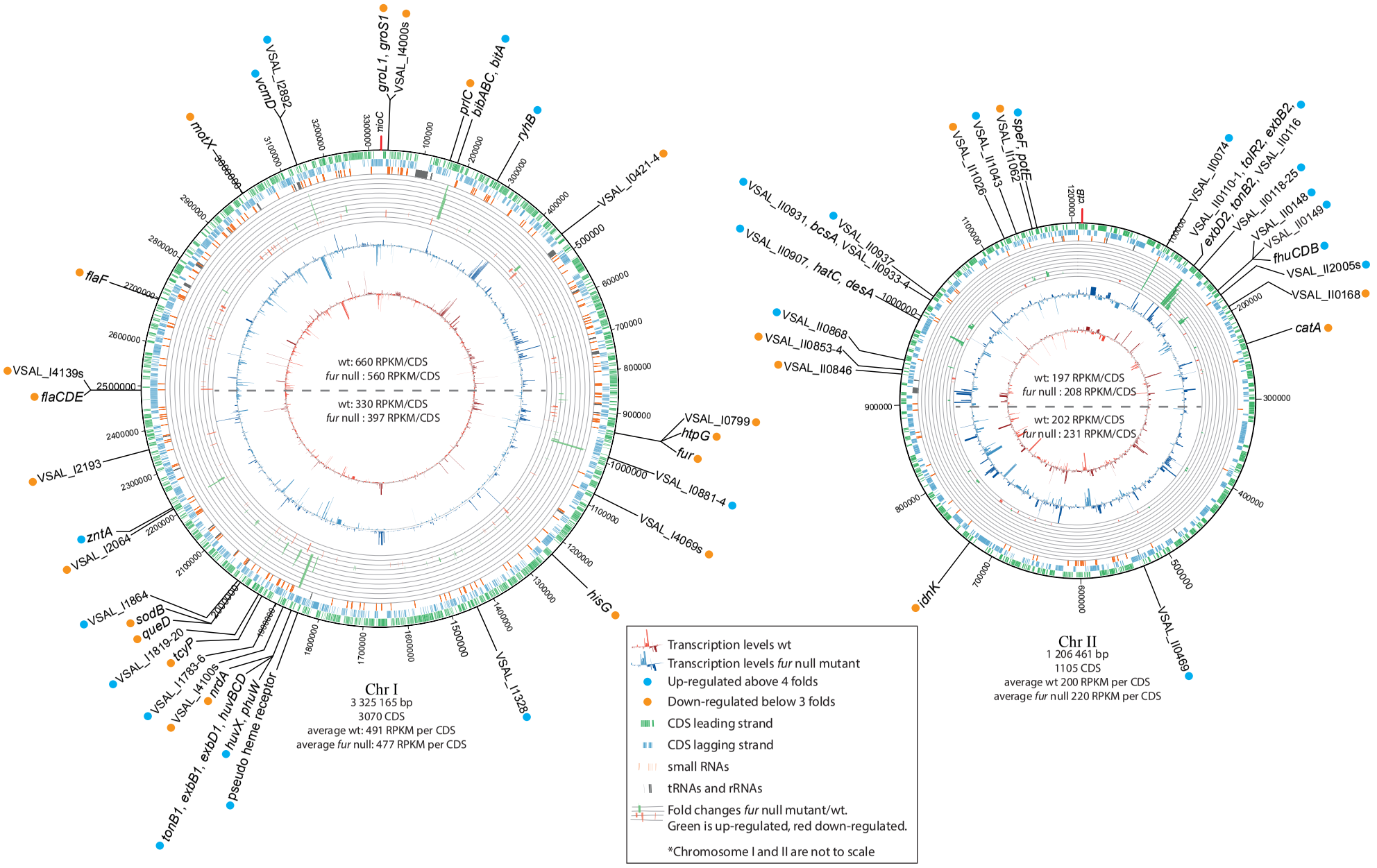
wt: 660 RPKM/CDS
fur null : 560 RPKM/CDS
wt: 330 RPKM/CDS
fur null : 397 RPKM/CDS
Chr I
3 325 165 bp
3070 CDS
average wt: 491 RPKM per CDS
average fur null: 477 RPKM per CDS
wt: 197 RPKM/CDS
fur null : 208 RPKM/CDS
wt: 202 RPKM/CDS
fur null : 231 RPKM/CDS
Chr II
1 206 461 bp
1105 CDS
average wt 200 RPKM per CDS
average fur null 220 RPKM per CDS
Transcription levels wt
Transcription levels fur null mutant
Up-regulated above 4 folds
Down-regulated below 3 folds
CDS leading strand
CDS lagging strand
small RNAs
tRNAs and rRNAs
Fold changes fur null mutant/wt.
Green is up-regulated, red down-regulated.
*Chromosome I and II are not to scale
groL1, groS1
VSAL_I4000s
prlC
bibABC, bitA
ryhB
VSAL_I0421-4
VSAL_I0799
htpG
fur
VSAL_I0881-4
VSAL_I4069s
hisG
VSAL_I1328
VSAL_I2892
vcmD
motX
flaF
VSAL_I4139s
flaCDE
VSAL_I2193
zntA
VSAL_I2064
VSAL_I1864
sodB
queD
VSAL_I1819-20
tcyP
VSAL_I1783-6
VSAL_I4100s
nrdA
tonB1, exbB1, exbD1, huvBCD
huvX, phuW
pseudo heme receptor
VSAL_II0931, bcsA, VSAL_II0933-4
VSAL_II0907, hatC, desA
VSAL_II0868
VSAL_II0853-4
VSAL_II0846
idnK
VSAL_II0469
VSAL_II1026
VSAL_II1043
VSAL_II1062
speF, potE
gdh
VSAL_II0074
VSAL_II0110-1, tolR2, exbB2, exbD2, tonB2, VSAL_II0116
VSAL_II0118-25
VSAL_II0148
VSAL_II0149
fhuCDB
VSAL_II2005s
VSAL_II0168
catA

Figure S1

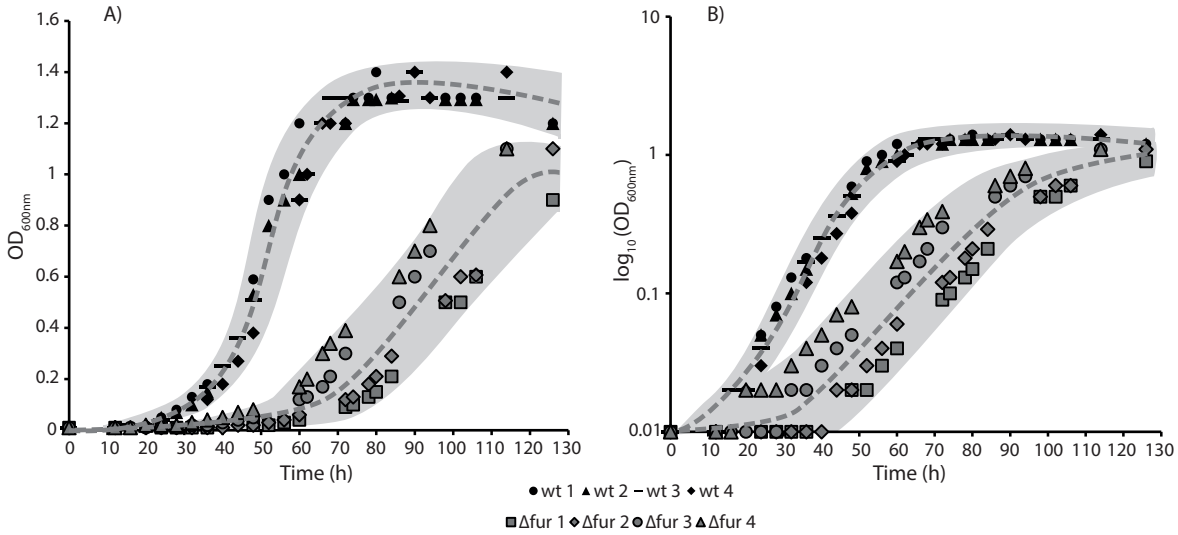
A)
B)
OD600nm
log10 (OD600nm)
Time (h)
Time (h)
wt 1 wt 2 wt 3 wt 4
Δfur 1 Δfur 2 Δfur 3 Δfur 4

Figure S2

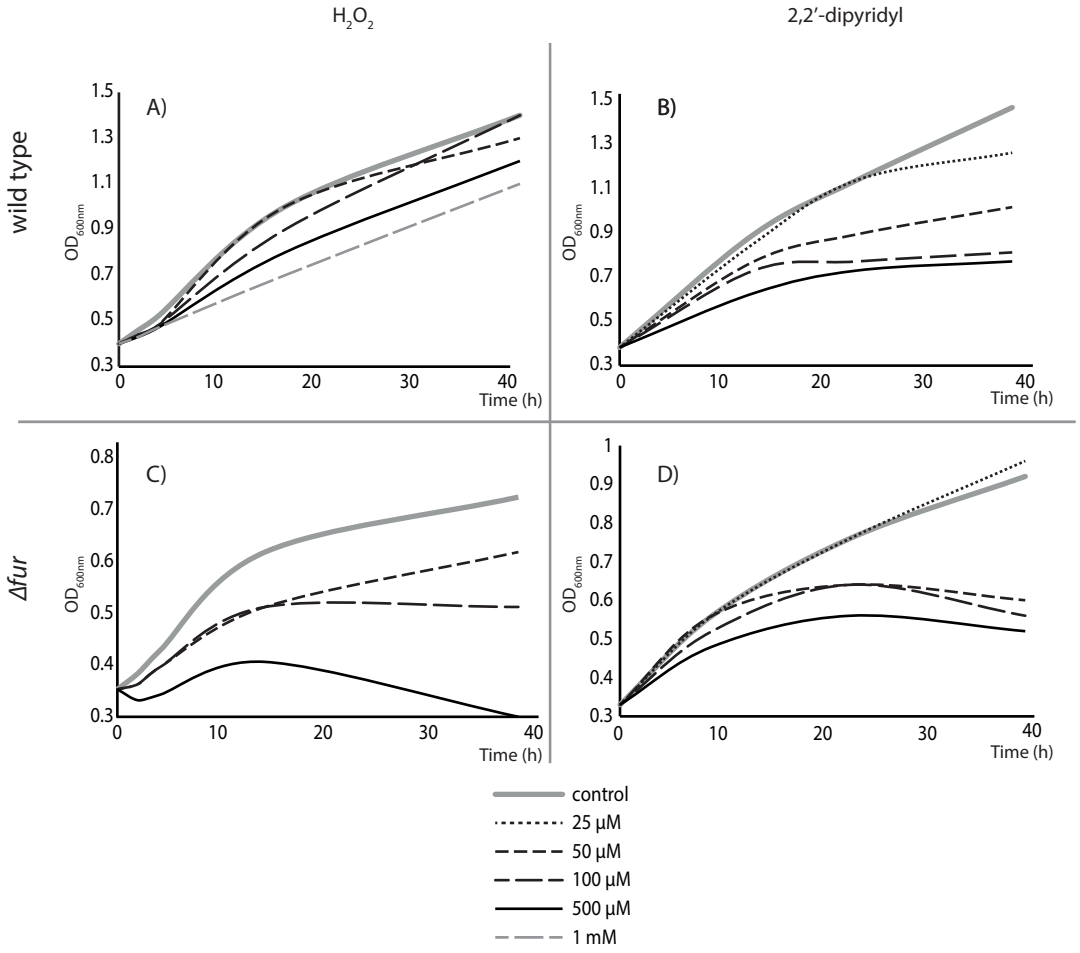
H2O2
2,2′-dipyridyl
wild type
Δfur
A)
B)
C)
D)
OD600nm
Time (h)
control
25 µM
50 µM
100 µM
500 µM
1 mM